Prediction and Measurement of Natural Vibrations of Multistage Launch Vehicles

VERNON L. ALLEY JR.[1] AND SUMNER A. LEADBETTER[2]

NASA Langley Research Center, Langley Air Force Base, Va.

The results of an analytical and experimental study to determine the first three natural frequencies of a four-stage research rocket are presented. A matrix recurrence equation is given which provides a convenient means for solving for the fundamental and higher modes of oscillation of the structure. Vibration tests were performed in a vertical fixture that afforded good unrestrained characteristics in one plane of motion. The results of studies of the effects of looseness in interstage connections, the unsymmetric behavior of a supposedly symmetrical structure, nonlinear characteristics, and an empirical treatment of joint flexibility are discussed. Good agreement between the calculated and measured data is shown.

Nomenclature

$[B]$ = matrix of mass characteristics
c_u = coordinate about the x origin to joint u, in.
$[D(s)]$ = special sweeping matrix for the sth mode
E = modulus of elasticity, psi
I = moment of inertia of structural cross-sectional area, in.^{4}
L = overall length of the vehicle, in.
m = total mass of the system $= \sum_{r=0}^{p-1} m_r$, lb-sec^2/in.
m_r = rth discrete mass, lb-sec^2/in.
m_x = mass distribution per inch of length, lb-sec^2/in.^{2}
n = number of the highest mode sought in the solution
p = number of discrete masses representing the system
$\bar{r}$ = radius of gyration of the system about the center of gravity, in.
v = total number of elastic joints considered in the system
x = coordinate having its origin at the center of the zeroth mass, in.
x_r = x coordinate to the rth discrete mass, in.
$\bar{x}$ = distance to the center of gravity of the total discrete mass system from the x origin, in.
y_r = displacement of the rth mass, in.
y_L = tip deflection used for normalizing mode data, in.
$y_r(s)$ = rth coefficient of the modal column for the sth mode, in.
z = parallel coordinate system to x having its origin at the aftermost point of the vehicle, in.
$\alpha_{i,j}$ = deflection influence coefficient for beam deflection only; deflection at $x = x_i$ due to a unit load at $x = x_j$ when cantilevered at $x = 0$, in./lb.
$\delta_{i,j}(u)$ = deflection influence coefficient considering elastic rotation of joint u only; deflection at $x = x_i$ due to a unit load at $x = x_j$ when cantilevered at $x = 0$, in./lb
κ_u = joint rotation constant for joint u, rad/in.-lb
$\sigma_{r,n}$ = total deflection influence coefficient considering beam and joint contributions; deflection at $x = x_r$ due to a unit load at $x = x_n$ when cantilevered at $x = 0$, in./lb
ω_s = circular frequency for vibrations of the sth free-free natural mode, rad/sec

Matrix notation

{ }, [ ], [ ], [ ], [1] designate column, diagonal, square, row, and unit matrices, respectively

Presented at the ARS Launch Vehicles: Structures and Materials Conference, Phoenix, Ariz., April 3–5, 1962.

[1] Aero-Space Technologist.

[2] Aero-Space Technologist.

IN the design of slender multistage boosters for upper atmospheric and space research probes, the accurate determination of the natural vibrations of the structure for flight conditions is an essential effort in the engineering program. Many of these vehicles are spin stabilized to prevent the vehicle from executing undesirably large dispersions with respect to the programmed trajectory. Spinning of the vehicle, however, introduces the possibility of incurring resonance or near resonant vibrations during flight. The high dynamic loads that result from spin resonance combined with the many other loads that a vehicle normally encounters in atmospheric flight would be a sure cause of failure for most highly optimized structures.

Frequently, an accurate knowledge of the natural frequencies, including experimental verification, is desirable in vehicles where the spin stabilization programs with their wide tolerances in spin rate fall in the narrow band between the short-period aerodynamic frequency and the first natural frequency of body bending. In addition, an understanding of the inherent frequencies that are likely to be experienced in the structure is of value in establishing proper instrumentation for monitoring environmental responses. Modal information is also essential to proper positioning of guidance sensing devices and for investigating the stability characteristics of vehicles with closed loop control systems. The orthogonal properties of the mode shapes make them desirable functions for use in series solutions involving generalized coordinates, widely known as "modal form solutions."

The transient mass and structural characteristics of a typical multistage rocket vehicle require that natural mode evaluations be made, at least for the ignition and burnout times of each stage of flight and frequently at other points of investigation, such as Mach 1, maximum dynamic pressure, and minimum stability. Transient wind response studies developed around modal form solutions that consider variable coefficients in the equations of motion frequently require that the natural modes and their related properties be defined as often as 10 times during first-stage flight. These stringent requirements involve substantial engineering effort and thereby justify the development and organization of adequate techniques for calculating modal data. They also emphasize the importance of performing experimental investigations to ascertain the suitability of the methods used.

In this paper, equations of motion are presented for the free-free natural vibrations of rocketlike structures, and results of the application of the equations to an actual four-stage space test vehicle are given. The analytical procedure consists of a matrix formulation that permits the coordination of

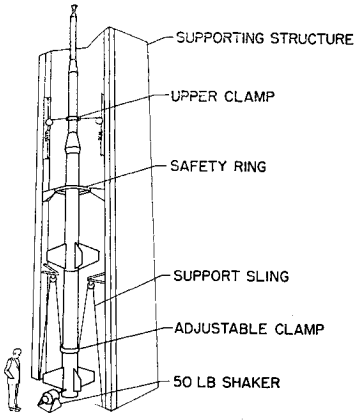

Fig. 1 Principal features of test apparatus

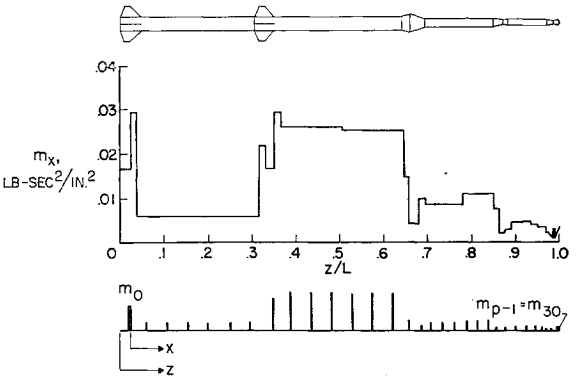

Fig. 2 Vehicle mass distribution

many computational stages into a single matrix equation from which the frequencies and mode shapes of the system can be obtained.

A comparison between the calculated and measured natural frequencies and mode shapes is furnished. Consideration is also given, in the experimental test program, to the lack of symmetry in a supposedly symmetrical vehicle, the linearity of response, structural damping, and the influence of looseness in the screwed joints.

Apparatus and Test Procedure

Description of Apparatus

Test vehicle

The full-scale four-stage solid propellant vehicle shown in Fig. 1 was used as the test specimen. All of the rocket types have been used, either individually or in combination in aerospace research probes. The test vehicle was made of the following rockets: first stage, Lance; second stage, Lance; third stage, Recruit; fourth stage, T-55.

The condition studied was burnout of the first stage. The second and third stages of the test vehicle were loaded with an inert mass having about the same density and stiffness as the solid fuel. Concentrated masses were added to the fourth stage to simulate the fuel and instrumentation. The interstage structural connections and separation devices employed in the test vehicle were one-piece, externally threaded, flanged bulkheads, generally referred to as blowout diaphragms. The stages are thus threaded together upon the separation diaphragms. The effects of the looseness of these interstage connectors on the natural frequencies of the system were studied as part of the investigation.

Test stand

The suspension system shown in Fig. 1 was constructed so that the vehicle, when placed in the vertical attitude, could approach the unrestrained condition of free flight in one plane. An adjustable clamp, supported by two cables located in a longitudinal plane of the vehicle and positioned at or near the lower nodal point, supported the vehicle's weight without contributing a significant restraint to motions normal to the plane of the cables. An upper support stabilized the vehicle in the upright position and was composed of two spring-loaded cables running normal to the vehicle's centerline and in the plane of the lower support cables. This support was located at or near an upper nodal point. During the tests it was found that the upper support could be loosened and the vehicle easily could be held vertically by holding it by hand at the upper nodal point.

Shaker system

A 50-lb vector force electromagnetic exciter was connected to the vehicle at a point $10\frac{1}{2}$ in. from the bottom of the first stage, as shown in Fig. 1. The exciter proved to be well matched to the vehicle for purposes of driving the first three natural modes of the system.

Instrumentation

Eight strain-gage accelerometers were located along the length of the vehicle, two on each stage near the junctions, to measure displacements at the stations. The outputs from the accelerometers were fed through amplifiers to an oscillograph recorder for permanent records of the vibration data. The accelerometer data were reduced to obtain the natural frequencies, mode shapes, and structural damping of the vehicle. The accelerometers were attached to an adapter designed in such a manner that a cavity between the adapter and the vehicle could be evacuated with a vacuum pump to enable the accelerometer to be held in place by means of atmospheric pressure.

Test Procedure

The first three mode shapes and the corresponding frequencies of the vehicle were determined with the lower suspension support or clamp at two different station locations (tests 1 and 2) and with the vehicle rotated 90° about the axis of symmetry from the original condition (test 3). The latter test was conducted to investigate the possibility that allowable tolerances in machining mating parts and fabrication tolerances might result in unsymmetrical bending stiffness of the joints. Theoretically, in all aspects, the vehicle was designed to be symmetrical about the longitudinal axis.

Measurements were also made to determine the effects of joint tightness and amplitude of oscillation on the frequency of the first natural mode with the vehicle suspended as during test 3. In order to study the effects of joint looseness, vibration tests were made with the joints between the first and second stages unwound by increments to 80° of relative rotation. The stages separated at the rate of 0.00046 in./deg of rotation.

The accelerometer on the first stage nearest the exciter was employed as the control instrument and was used to define the amplitude of oscillation. The damping coefficient was determined by observing the decay of the vibrations.

Vehicle Structural Properties

The optimum strength-weight requirements on space vehicles result in highly complicated structures whose mass and stiffness distributions are difficult to establish. In Fig. 2 the mass per inch parameter of the test vehicle is plotted against the normalized axial coordinate z/L. These data illustrate the severe lack of symmetry and the wide departure of the typical launch vehicle from the uniform distribution. The total weight of the vehicle as tested was 2687 lb. Two coordinate systems are referred to in this paper and are indi-

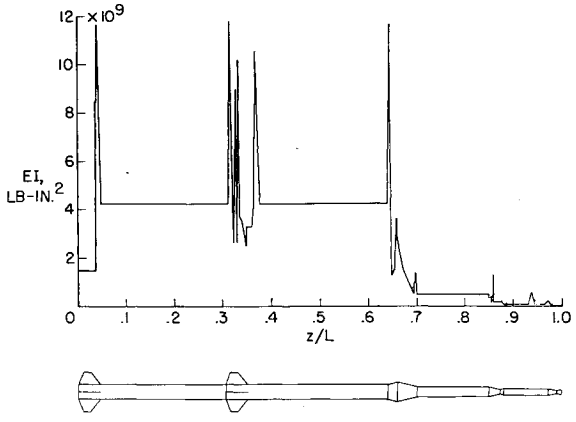

Fig. 3 Vehicle flexural stiffness distribution

cated on Fig. 2. The z coordinate defines distances along the length of the vehicle from the aftermost point, and the x coordinate is parallel to z but has its origin at $z = 13.36$ for the test vehicle. The x origin is the center of the first mass (m_0) of the equivalent discrete mass system used in the analysis.

In Fig. 3, the discontinuous and highly variable nature of the flexural stiffness coefficient EI is shown. These data illustrate the typical complexity of rocket structures and the degree of definition used in defining the function for an accurate calculation of the natural modes and frequencies. The transition sections between the standard rocket motors are the most difficult regions to define and generally are the spaces that contribute a major part to the flexibility. In computing the EI data of Fig. 3, all changes in diameter of the load carrying structure were considered mechanically without modifications or devising equivalent systems. In regions where this technique failed to express adequately the nature of the flexure, rotation constants were employed which are discussed in a subsequent section.

Analytical Procedures

Equations of Motion

The analytical process that was used for computing the theoretical frequencies and mode shapes for the study is derived and discussed in detail by Alley and Gerringer.[3] The analysis is developed around a discrete mass representation of the continuous system and the load-deflection relationships are equated by use of deflection influence coefficients. The inherent nature of the discrete mass-influence coefficient type of problem makes it ideal for matrix notation, and the use of matrices permits the expression of a single final equation from which both the frequencies and natural mode shapes can be obtained. The following equation, obtained from Eq. [20] of the paper by Alley and Gerringer, is the general matrix expression from which both the fundamental and higher natural modes of vibration were computed by matrix iteration.

$$(1/\omega_s^2 m)\{y_r(s)\} = [B][\sigma_{r,n}][m_r/m][D(s)]\{y_r(s)\} \qquad [1]$$
$$r = 1, 2, 3 \ldots p - 1$$

where the various parametric matrices are defined as follows:

$$[B] = \left[[1] + \left[\frac{\bar{x}^2}{\bar{r}^2} \left\{ \frac{x_r}{\bar{x}} \right\} \left[1 - \frac{x_r}{\bar{x}} \right] - \{1\} \left[1 + \frac{\bar{x}^2}{\bar{r}^2} - \frac{\bar{x}^2}{\bar{r}^2} \frac{x_r}{\bar{x}} \right] \right] [m_r/m] \right]$$

$[\sigma_{r,n}]$ = influence coefficient matrix

$[m_r/m]$ = mass matrix

$$[D(s)] = \left[[1] - \frac{\{y_r(1)\}[y_r(1) - y_0(1)][m_r/m]}{[y_r(1) - y_0(1)][m_r/m]\{y_r(1)\}} - \frac{\{y_r(2)\}[y_r(2) - y_0(2)][m_r/m]}{[y_r(2) - y_0(2)][m_r/m]\{y_r(2)\}} \cdots - \frac{\{y_r(s-1)\}[y_r(s-1) - y_0(s-1)][m_r/m]}{[y_r(s-1) - y_0(s-1)][m_r/m]\{y_r(s-1)\}} \right]$$

and

$$y_r(s = 0) = 0$$

Eq. [1] is a recurrence equation in that, if the sth natural mode and frequency are desired, the $s = 1$ through $s - 1$ modes must have been previously determined. If the number of discrete masses representing the system is p, then the order of the given matrices is $p - 1$. There are $p - 1$ linearly independent eigenvectors, of which $p - 2$ are the flexible mode shapes, and one, associated with a zero eigenvalue, has no physical significance. The B matrix is a distinct function of the mass characteristics of the system. The $\sigma_{r,n}$ matrix contains the basic flexural relationships of the system. The $D(s)$ matrix is a special sweeping matrix appropriate to the specific orthogonality relationships of the modal columns. The orthogonality relationships differ from most other similar solutions because the modal columns are not complete for the system in that $y_{r=0}$ is omitted. The orthogonality relationship applicable to the incomplete modal column is

$$[y_r(i) - y_0(i)][m_r/m]\{y_r(j)\} = 0 \qquad i \neq j \qquad [2]$$

and the omitted end displacement $y_0(i)$ from the modal column $y_r(i)$ is readily obtained by

$$y_0(i) = -\frac{1}{m_0/m}[1][m_r/m]\{y_r(i)\} \qquad [3]$$

where y_0 fails to appear in the modal column, since the origin of the x coordinate system and the reference for the influence coefficients are taken at the position of m_0. This selection for the position of the x origin is advantageous in that it reduces the order of the matrices to $p - 1$ for a system having p masses.

Number of Discrete Masses

The number of masses used in Eq. [1] should be based primarily on the accuracy desired for the highest mode to be extracted and the capability of available computing equipment to handle large matrix iterations. The results of a study of the influence of the number of masses on the errors in frequency and mode shapes of a uniform free-free beam are given in the paper by Alley and Gerringer. It was found that, for the first five modes, errors in frequency resulting from lumping mass can be held to within 1% by the use of the following approximate rule: $p = 13(n)^{1/3}$, where n is the number of the highest mode desired and p is the number of masses to be used. This rule is stated to afforded an approximate guide for establishing the number of masses to be used in calculating asymmetrical beam systems such as the rocket vehicle considered in this paper. The computed modal data submitted with this report were calculated considering 31 discrete masses ($p = 31$). This number should effectively remove all significant lumping errors from the computed data.

Influence Coefficients

The influence coefficients $\sigma_{r,n}$ required in Eq. [1] must be cantilever beam influence coefficients fixed at the x origin. The appropriateness of the influence coefficients in represent-

[3] Alley, V. L., Jr. and Gerringer, A. H., "A matrix method for the determination of the natural vibrations of free-free unsymmetrical beams with application to launch vehicles," NASA TN D-1247 (1962).

ing the actual structure will depend largely upon the skill of the analyst in interpreting the structural plans and the inclusion of secondary effects when necessary. The influence coefficients used in the determination of the calculated data for this paper were computed by consideration of elementary beam flexure with the addition of local rotations due to joints. The influence coefficients were expressed in two parts:

$$\sigma_{i,j} = \alpha_{i,j} + \sum_{u=1}^{u=v} \delta(u)_{i,j} \qquad [4]$$

where $\alpha_{i,j}$ is that portion of the influence coefficient resulting from beam flexure only and given by

$$\alpha_{i,j} = \int_0^{xi} \frac{x^2}{EI}\,dx - (x_j + x_i) \times \int_0^{xi} \frac{x}{EI}\,dx + x_i x_j \int_0^{xi} \frac{1}{EI}\,dx \qquad j \geq i \qquad [5]$$

and $\delta(u)_{i,j}$ is the contribution to the influence coefficient due to local rotation of the uth joint of which there are v such joints. It is given by

$$\delta(u)_{i,j} = \kappa_u(x_j - c_u)(x_i - c_u) \quad \text{valid when } x_i,\ x_j > c_u \qquad [6]$$
$$= 0 \text{ when } x_i,\ x_j \leqq c_u$$

The influence coefficients applicable to the specific problem are obtained by a point-by-point summation of deflections due to the rotation of the joints and the deflections resulting from flexure of the structure. The use of Maxwell's reciprocal law $\sigma_{i,j} = \sigma_{j,i}$ substantially reduces the necessary computations.

From Eq. [5] it can be seen that the evaluation of the influence coefficients will involve the determination of the integrals of the functions x^2/EI, x/EI, and $1/EI$. In most actual applications, these integrals must be determined by numerical integration. Results of an investigation of the error in the natural frequencies of a uniform beam which may be associated with the use of trapezoidal integration are given in the forementioned paper by Alley and Gerringer (see footnote 3). It was found that the integration errors introduced by the trapezoidal process tend to counteract the errors introduced by the discrete mass analogy, and it was indicated that the maximum size of the integration interval should not exceed $\frac{1}{50}$ of the vehicle's length.

Joint Rotation Effects

It has been observed in many rocket vehicles that significant local contributions to flexure frequently originate at joints and that these joint effects must be included in analyses involving flexure. Contributions of the joints to the deflections generally defy rigorous analytical description. Such contributions are consistently encountered from looseness in screwed joints, thread deflections, flange flexibility, plate and shell deformations that are not within the confines of beam theory, etc. Since it is generally impractical to evaluate these effects analytically, the problem has been treated empirically at NASA Langley Research Center with satisfactory results in the determination of natural vibration characteristics and aeroelastic problems. From limited measurements and observations of the inordinate behavior of typical rocket vehicle joints, the order of magnitude of rotations resulting from moment loading have been noted and recorded as "joint rotation constants." These constants κ_u are defined as the measure of the local rotation of the structure due to the application of bending moment, radians per inch-pound.

Admittedly, many typical local deflections are highly inordinate and nonlinear, and, for such cases, the linear empirical approach can only hope to provide an equivalent effect. Also, experience has shown that considerable variation in the behavior of similar joint designs can result from variation in fabrication skill. However, it should be kept in mind that estimates of κ_u are approximations to what should normally be a secondary influence in a good design, and it is upon this premise that such empirical means have been employed resulting in consistently improved accuracy of modal data. Invariably, computed mode data on rocket vehicles which disregard such local influences will result in frequencies higher than actual; therefore, any reasonable approximation to joint behavior will move the computed results in the proper direction. Nevertheless, the possibility of assuming joint factors unreasonably large does exist, and consequently such efforts may result in greater errors than would be experienced if totally ignored. A guide to joint evaluation which should provide a simple means for approximating the joint rotation constants in a typical rocket vehicle is submitted as Fig. 4. A variety of typical rocket vehicle joints are illustrated and classified from excellent to poor in light of their stiffness on Fig. 4a. Repeated experiences with bending resulting from local joint rotations has led to the classification shown. The curves of Fig. 4(b) were constructed around 10 measured quantities of κ_u for a variety of different classes of joints. Because of the limited quantity of measured data, the curves that show the variation in κ_u with diameter were not empirically established but were based on the assumption that κ_u is inversely proportional to the third power of the diameter. This is in accordance with the theoretical variation in flexibility of geometrically similar joints, and the resulting curves proved to be in good agreement with the measured data. Information of the type of Fig. 4 is primarily useful to designers who repeatedly are using the same types of joints in a variety of rocket vehicle assemblies.

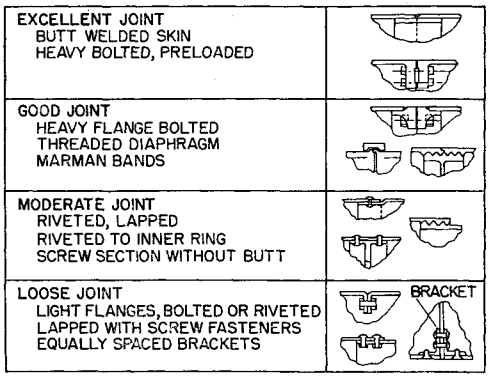

Fig. 4a Schematic diagrams of various types of joints

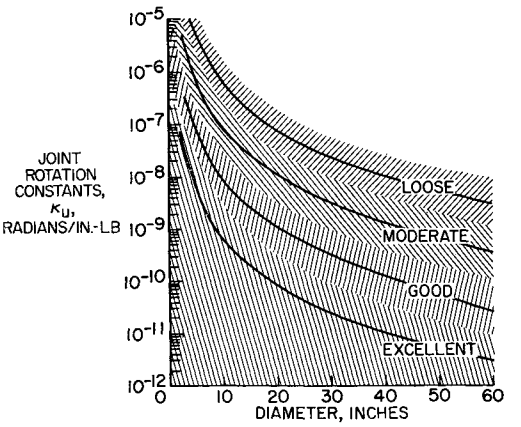

Fig. 4b Joint rotation constants

It is improbable that the factors contributing to so-called joint rotation effects will ever be completely amenable to analytical treatment, which leaves, then, two major avenues of approach to their solution: first and most appropriate, to design structures to avoid most of the geometries that defy analysis and permit inordinate behaviors; and second, as a

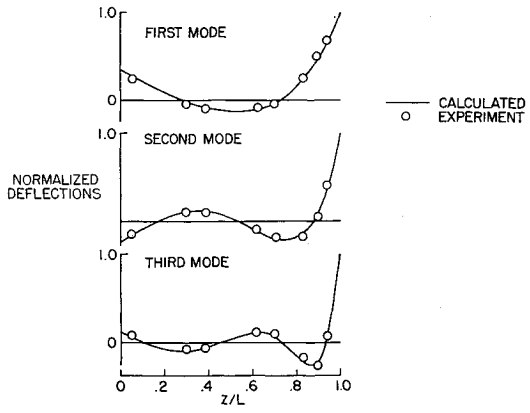

Fig. 5 Comparison of experimental and calculated natural mode shapes

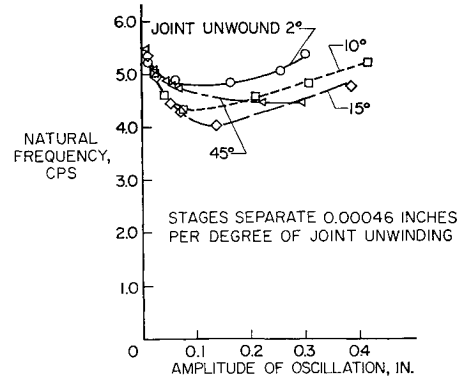

Fig. 7 Variation of natural frequency of first mode with joint looseness and amplitude of oscillation

last resort, to use empirical joint rotation data such as submitted in Fig. 4 for various classes of fabrications.

The data submitted as Fig. 4 are from limited observations, and considerable improvement in this approach should result from a finer classification of hardware and from a greatly increased sampling of joint data.

Results and Discussion

Presentation of Results

Typical results of the experimental measurements and the analytical study of the first three natural mode shapes of the four-stage test vehicle are presented in Fig. 5. The experimentally and analytically determined frequencies of the first three natural modes are presented in Fig. 6. The results of an experimental study of the effects of joint looseness on the response of the test vehicle are presented in Figs. 7 and 8. The damping coefficient, which is the familiar structural damping coefficient g defined as the ratio of twice the equivalent viscous damping to the critical damping, was determined also for the vehicle for the outputs of the accelerometers during the decay of the oscillations and was found to be of the expected magnitude, namely, in the order of 0.04, 0.05, and 0.06 for the first, second, and third modes, respectively.

Comparison of Experimental and Analytical Results

Typical results of the experimental and analytical studies of the first three mode shapes are shown in Fig. 5. The data are presented on a plot having the normalized deflection as the ordinate and the normalized length of the vehicle as the abscissa. The analytically determined mode shapes are indicated by the solid curves, and the normalized experimentally determined deflections are shown as the open symbols. Tests were conducted with various driving forces, support locations, and with the driving force applied in either the normal or transverse plane. The results show that the computed mode shape is in excellent agreement with the measured mode shapes for all test conditions. Neither the magnitude of the driving force, the location of the lower support, nor the rotation of the vehicle about its longitudinal axis had any appreciable effect on the first two mode shapes. It was observed, however, that there was a small deviation between the measured and calculated third mode shape in the upper stage when the vehicle was rotated 90°.

The results of the experimental and analytical study of the first three natural frequencies are shown in Fig. 6. The data are presented in tabular form showing a comparison of calculated frequency to the average measured frequency for the three test conditions. The average of the first mode frequencies determined in all test conditions differed from the calculated frequency by less than 1%. For all cases measured, there was a spread in the test data of 2%. The agreement of the test 2 results, where the position of the lower support was nearly ideal, was excellent. The frequency of the vehicle for the same support position, but with the vehicle rotated 90° about its longitudinal axis, was within 2% of the calculated value.

The average measured frequency for the second mode was about 8% lower than the calculated values. There was a spread of 4% in the measured natural frequencies of the second mode. The second mode test results supported the findings in the first mode studies of different vibration characteristics for motions in longitudinal planes normal to each other. A 3% reduction in second-mode frequency was observed in test 3 for the vehicle rotated 90° about its longitudinal axis.

The average measured frequency of the third mode was 12% lower than the calculated. There was a spread of 18% in the value of the experimentally determined frequencies. The lack of symmetry for oscillations in longitudinal planes normal to each other was quite apparent in the third mode. A 12% reduction in the third-mode frequency was recorded

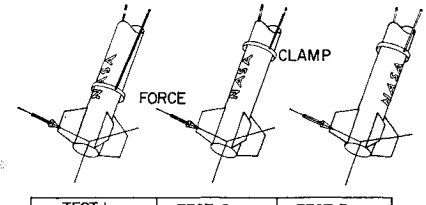

MODE	CALCULATED FREQUENCIES	TEST 1	TEST 2	TEST 3
		EXPERIMENTAL FREQUENCIES		
1	5.46	5.41	5.46	5.36
2	11.45	10.54	10.62	10.33
3	19.82	17.22	18.24	15.88

(ALL FREQUENCIES GIVEN IN CYCLES PER SECOND)

Fig. 6 Comparison of experimental and calculated natural frequencies for three test conditions

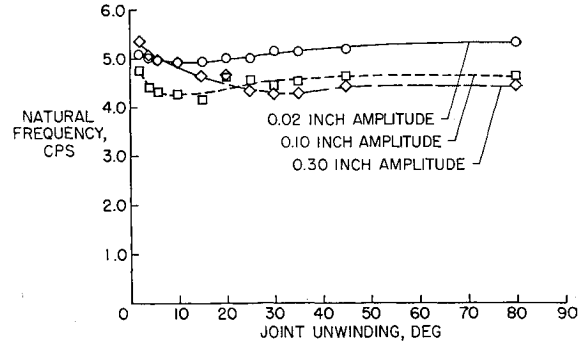

Fig. 8 Variation of natural frequency of first mode with joint looseness and amplitude of oscillation

in test 3 when exciting the vehicle normal to the test plane of tests 1 and 2. The reduction in frequency for motions in the 90° plane was consistent for all three modes. A shift in third-mode frequency of approximately 6% was attributed to changing the lower support location. It was observed consistently that all modes displayed decreases in frequency as the lower support position was moved toward the nodal points of the modes.

The observed variations in the measured values of the natural frequencies are probably due to the nonlinearities of the vehicle and limitations on obtaining sharp peak responses of the build-up structure.

The high length-to-diameter ratio of the test vehicle implements the belief that, for the three modes investigated, rotary inertia and shear omissions in the calculations could hardly account for the difference observed in the frequencies of the second and third modes. Furthermore, the errors introduced by the process of lumping the masses are unlikely the source, since such effects should be well below 1%. The previously mentioned rule, $13(n)^{1/3}$, for determining the number of masses compatible with a 1% error indicated that 19 masses would have been sufficient for controlling errors to within 1%. The use of 31 masses in the analysis should limit errors due to the discrete mass representation of the continuous system to considerably less than 1%.

It then appears that the differences between the measured and calculated natural frequencies are probably due to the inadequate analytical representation of the vehicle's stiffness properties. This is reasonable to expect in light of the extreme complexity of the structure of a typical space vehicle and always will be a fertile source of error which will vary considerably with the skill and intuition of the analyst. No generalization can be made as to the influence of inadequate representation of structural and mass characteristics on the various modes, since the significance of such discrepancies on a given mode depends strongly upon the location of such errors. For instance, an overlooked region of flexibility will not alter the frequency of a mode if it coincides with, or is near, an inflection point, but it can have a large effect on another mode where such favorable conditions do not exist.

It should also be noted that complicated structures of the type of the test vehicle frequently exhibit flexural nonlinearity to some degree. In comparing the measured results with the results of the calculations based on an assumed linear system, the best agreements are generally to be expected for the lowest amplitudes of oscillations. No strong correlation of this nature can be drawn, however, from the results of the tests reported herein, since the different levels of excitation effected increases in frequency with increases in driving forces in some cases and reduction in frequency in others. From the data presented and discussed in the following section, with looseness existing in the joint, the frequency-amplitude relationship appears to be of the expected behavior. The decrease in frequency with increase in the amplitude of oscillation for the low-level vibration is in agreement with the behavior of some nonlinear systems. Another indication of nonlinear system was exhibited, in tuning the system to a particular mode, by a jump from a high amplitude of oscillation to a lower amplitude as the frequency was varied. Care was taken in tuning the system to obtain the maximum amplitude of oscillations.

Effects of Joint Looseness and Amplitude of Oscillation

The effects of looseness in the screw joint between the second and third stages on the first natural frequency of the test vehicle are indicated on Fig. 7 as a function of amplitude of oscillation. The frequency data obtained for various amounts of joint looseness are shown as the open symbols with curves faired through the data to emphasize trends.

As the amplitude of oscillation (measured by the accelerometer nearest the exciter) is increased, the natural frequency at first decreases and then at larger amplitudes increases. This behavior is attributed to the nonlinear characteristics of the loose joint. For small amplitudes of oscillation, the weight of the upper stages holds the screw threads firmly in contact throughout a cycle, and the natural frequency is therefore essentially the same as for the tight joint. At larger amplitudes of oscillation, the joint is rocked back and forth through the free play of the loose threads, which results in an effective reduction in stiffness with a related reduction in frequency. For large amplitudes of oscillation, the backlash contribution to deflection becomes a secondary part of the total flexure, and the natural frequency approaches the initial value for the tight joint.

A cross plot of the data of Fig. 7 is presented as Fig. 8. These curves clearly show the variation in frequency with unwinding in the joint between the second and third stages of the vehicle. It is interesting to note that partial recovery in frequency is observed for the larger values of unwinding investigated.

Studies similar to those for which the results are given in Figs. 7 and 8 were made also for unwinding of the joint between the first and second stages of the test vehicle. The trends were in all respects similar to the variations observed for the joint between the second and third stages discussed previously.

Conclusions

As a result of the experimental and analytical investigation of the vibration characteristics of the four-stage solid propellant vehicle reported herein, the following conclusions can be made:

1) The results show that the averages of the measured natural frequencies are within 1, 8, and 12% of the calculated frequencies for the first, second, and third modes, respectively.

2) The mode shapes of the first three modes were accurately predicted by the analytical procedure presented.

3) Variations in the location of the lower suspension system clamp on the vehicle, in relation to the nodal points, did not appreciably affect the free-free natural mode shapes and frequencies for the first and second modes. A small sensitivity to its position was observed by the associated changes in the value of the third natural frequency.

4) With loose interstage connections, the frequency dependency upon amplitude is typical of the nonlinear behavior associated with systems having free play. As the amplitude is increased gradually, the natural frequency first decreases and then increases to the extent that, for the larger amplitudes tested, the frequency had increased almost to the values obtained for the tight system.

5) Reductions in the natural frequency of the first mode of up to 20% were noted during unwinding of the screw joints between the second and third stages. This natural frequency of the vehicle tended to decrease with initial unwinding of the screw joint between stages and then indicated a partial recovery toward its initial value for the larger angles of unwinding.

6) The structure, although designed to be geometrically symmetrical about the longitudinal axis, showed a small but consistent difference in the vibration characteristics of the first three modes for tests in longitudinal planes 90° with respect to each other. This unsymmetrical behavior indicates that the inherent influences of tolerances and fabrication effects might produce unpredictable variations in frequencies of several percent in theoretically similar vehicles.

7) It is felt that the differences between measured and computed frequencies primarily are due to the differences between the actual mass and stiffness of the vehicle and the corresponding values used in the computations. These parameters are difficult to define in complicated space vehicles and are subject to considerable variation due to the individual interpretation of the structural load paths.